

## Journal Pre-proofs

A bicyclic pentapeptide-based highly potent and selective pan-SIRT1/2/3 inhibitor harboring N<sup>ε</sup>-thioacetyl-lysine

Renwu Li, Lingling Yan, Xun Sun, Weiping Zheng

PII: S0968-0896(20)30147-4  
DOI: <https://doi.org/10.1016/j.bmc.2020.115356>  
Reference: BMC 115356

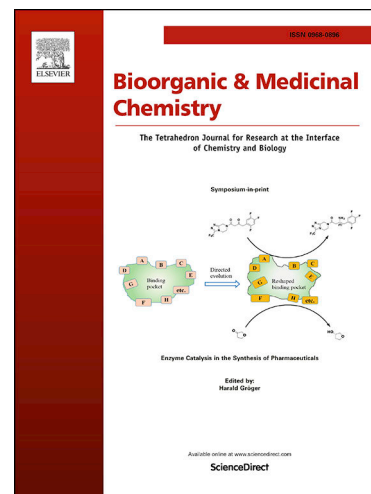
To appear in: *Bioorganic & Medicinal Chemistry*

Received Date: 13 November 2019  
Revised Date: 29 January 2020  
Accepted Date: 31 January 2020

Please cite this article as: R. Li, L. Yan, X. Sun, W. Zheng, A bicyclic pentapeptide-based highly potent and selective pan-SIRT1/2/3 inhibitor harboring N<sup>ε</sup>-thioacetyl-lysine, *Bioorganic & Medicinal Chemistry* (2020), doi: <https://doi.org/10.1016/j.bmc.2020.115356>

This is a PDF file of an article that has undergone enhancements after acceptance, such as the addition of a cover page and metadata, and formatting for readability, but it is not yet the definitive version of record. This version will undergo additional copyediting, typesetting and review before it is published in its final form, but we are providing this version to give early visibility of the article. Please note that, during the production process, errors may be discovered which could affect the content, and all legal disclaimers that apply to the journal pertain.

© 2020 Published by Elsevier Ltd.



## **A bicyclic pentapeptide-based highly potent and selective pan-SIRT1/2/3 inhibitor harboring N<sup>ε</sup>-thioacetyl-lysine**

Renwu Li <sup>a,§</sup>, Lingling Yan <sup>b</sup>, Xun Sun <sup>a,c,\*</sup>, Weiping Zheng <sup>b,¶,\*</sup>

*<sup>a</sup>Department of Natural Products Chemistry, School of Pharmacy, Fudan University, 826 Zhangheng Road, Shanghai 201203, P. R. China*

*<sup>b</sup>School of Pharmacy, Jiangsu University, 301 Xuefu Road, Zhenjiang 212013, Jiangsu Province, P. R. China*

*<sup>c</sup>Shanghai Key Laboratory of Clinical Geriatric Medicine, Shanghai 201203, P. R. China*

\* Correspondence: [wzheng@ujs.edu.cn](mailto:wzheng@ujs.edu.cn) (W. Zheng), [sunxunf@shmu.edu.cn](mailto:sunxunf@shmu.edu.cn) (X. Sun)

§ A visiting doctoral student at Zheng laboratory at Jiangsu University.

¶ lead contact.

## Abstract

Past few years have seen an active pursuit of the inhibitors for the deacylation catalyzed by the seven human sirtuins (i.e. SIRT1-7) as valuable chemical biological/pharmacological probes of this enzymatic deacylation and lead compounds for developing novel therapeutics for human diseases. In the current study, we prepared eight monocyclic and one bicyclic analogs of a linear pentapeptide-based potent (sub- $\mu\text{M}$   $\text{IC}_{50}$ 's) pan-SIRT1/2/3 inhibitor Zheng laboratory discovered recently that harbors the catalytic mechanism-based SIRT1/2/3 inhibitory warhead  $\text{N}^{\epsilon}$ -thioacetyl-lysine at its central position. We found that the bicyclic analog exhibited largely comparable SIRT1/2/3 inhibitory potencies to those of the parent linear pentapeptide, however, the former is proteolytically much more stable than the latter. Moreover, the bicyclic analog displayed very weak inhibition against SIRT5/6/7, was cell permeable, and exhibited an anti-proliferative effect on the human SK-MEL-2 melanoma cells. This bicyclic analog could be a lead for the future development of more potent and still selective pan-SIRT1/2/3 inhibitors whose use in studies on human sirtuin biology, pharmacology, and medicinal chemistry could complement with the use of the potent inhibitors selective for a single human sirtuin.

**Keywords:**  $\text{N}^{\epsilon}$ -thioacetyl-lysine; cyclic peptide; sirtuin; inhibitor; structure-activity relationship.

## 1. Introduction

Sirtuins refer to a family of intracellular proteins able to catalyze the  $\beta$ -nicotinamide adenine dinucleotide ( $\beta$ -NAD<sup>+</sup>)-dependent side chain deacylation of the N<sup>ε</sup>-acyl-lysine residues on their substrate proteins (Fig. 1)<sup>1-9</sup>. As also indicated in Fig. 1, the N<sup>ε</sup>-acyl groups can be acetyl and those bulkier ones<sup>1,2,4,5,7,8</sup>. The lysine side chain N<sup>ε</sup>-acylation on proteins can be accomplished by enzymatic or non-enzymatic reactions<sup>1,6,10-16</sup>. The sirtuin proteins are present in organisms from all the three evolutionary kingdoms of life, i.e. bacteria, archaea, and eukarya; and seven sirtuins (i.e. SIRT1-7) have been found thus far in mammals including humans<sup>17</sup>. The sirtuin-catalyzed deacylation has been increasingly demonstrated to play an important role in regulating a variety of crucial cellular processes such as transcription, metabolism, and DNA damage repair<sup>2,5,18-28</sup>. Also, this enzymatic deacylation has been regarded as a contemporary therapeutic target for developing novel therapeutics for human diseases such as cancer, neurodegeneration, and metabolic diseases<sup>29-32</sup>. As such, past

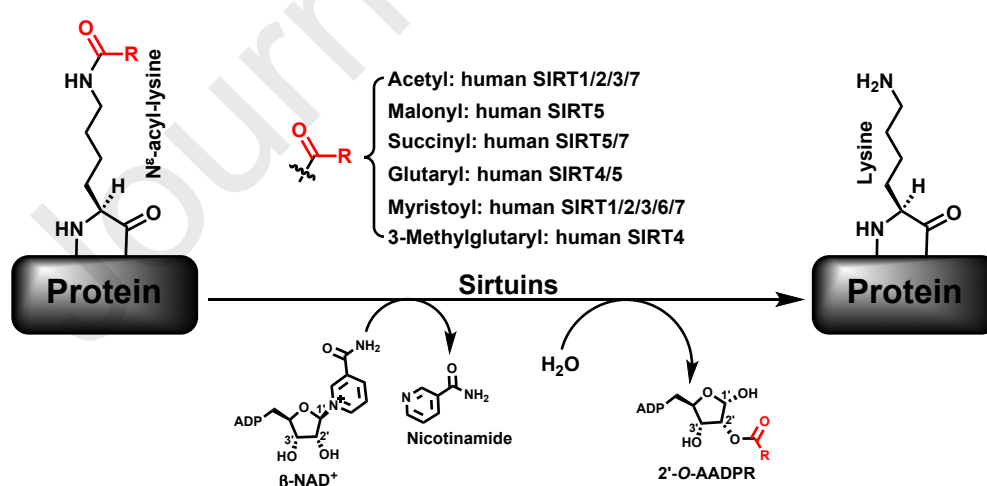


**Fig. 1.** The sirtuin-catalyzed  $\beta$ -NAD<sup>+</sup>-dependent deacylation of N<sup>ε</sup>-acyl-lysine protein substrates. Example R-C(=O)- removable by different human sirtuins are also indicated.

**Note:** The SIRT7-catalyzed deacetylation and demyristoylation can be promoted by dsDNA, rRNA, or tRNA.

few years have seen an active pursuit of the chemical modulators (inhibitors and activators) for the sirtuin-catalyzed deacylation as potential therapeutics and also as chemical probes for sirtuin biochemistry, biology, and pharmacology<sup>3,4,8,29,31-34</sup>.

As for the human sirtuin inhibitor development, while potent and selective inhibitors are the major type of molecular entities that have been pursued and have been thus far indentified for SIRT1, SIRT2, SIRT5, and SIRT6<sup>4,29,31-34</sup>, those potent pan-sirtuin inhibitors such as the potent and selective dual SIRT1/2 inhibitors Zheng laboratory recently identified<sup>35</sup> may also have their unique appeal in that their use in the studies on human sirtuin biology, pharmacology, and medicinal chemistry could complement with the use of the potent inhibitors selective for a single human sirtuin. In the current study, we discovered a N<sup>ε</sup>-thioacetyl-lysine-containing bicyclic pentapeptide (i.e. compound **10** in Fig. 2) as a potent (sub- $\mu$ M IC<sub>50</sub>'s) pan-inhibitor selective for human SIRT1/2/3 (*versus* human SIRT5/6/7).

## 2. Materials and Methods

### 2.1. General

The following were purchased for the compound preparation and were used as received from commercial vendors without further treatment. Sigma-Aldrich China:

N-methylmorpholine (NMM), trifluoroacetic acid (TFA), N,N-dimethylformamide (DMF), anhydrous tetrahydrofuran (THF); TCI Shanghai: 4-bromobutyric acid, 6-bromohexanoic acid, 1,8-diazabicyclo[5.4.0]undec-7-ene (DBU), 1,1,1,3,3,3-hexafluoroisopropanol (HFIP), 3-bromopropylamine hydrobromide; Enamine Ltd.: 7-bromoheptylamine hydrobromide; Alfa Aesar China: 11-bromoundecanoic acid, sodium iodide (NaI), sodium methoxide (MeONa),

phenol, thioanisole, ethanedithiol, N-hydroxybenzotriazole (HOBt),  
2-(1H-benzotriazole-1-yl)-1,1,3,3-tetramethylammonium hexafluorophosphate (HBTU),  
2-(7-aza-1H-benzotriazole-1-yl)-1,1,3,3-tetramethyluronium hexafluorophosphate (HATU),  
*N,N*-diisopropylethylamine (DIPEA); J&K Scientific Ltd.: 8-bromooctanoic acid;  
Honeywell China: acetonitrile, dichloromethane (DCM), methanol (MeOH), hexanes;  
Sinopharm Chemical Reagent Co., Ltd.: piperidine, diethyl ether, acetic anhydride; Shanghai  
Plus Bio-Sci & Tech Co., Ltd.: Rink amide 4-methylbenzhydrylamine (MBHA) resin; GL  
Biochem (Shanghai) Ltd.: 2-chlorotriyl chloride resin.

$N^{\alpha}$ -9-Fluorenylmethoxycarbonyl (Fmoc)- $N^{\epsilon}$ -thioacetyl-lysine was synthesized from  
 $N^{\alpha}$ -Fmoc-lysine hydrochloride (purchased from TCI Shanghai) and ethyl dithioacetate  
(purchased from Sigma-Aldrich China) according to the procedure Zheng laboratory  
previously reported<sup>36</sup> and was used in the current study for incorporating  $N^{\epsilon}$ -thioacetyl-lysine  
into compounds **2-10**. All the other  $N^{\alpha}$ -Fmoc-protected amino acids were purchased from the  
following commercial vendors: Sigma-Aldrich China, Alfa Aesar China, TCI Shanghai, GL  
Biochem (Shanghai) Ltd., or Chem-Impex International Inc.

Routine unit-resolution mass spectrometry (MS) was performed with a Thermo LXQ  
LC-ion trap mass spectrometer at Jiangsu University. High-resolution mass spectrometry  
(HRMS) was performed with an AB 5600+ Q TOF high-resolution mass spectrometer at the  
Pharmacy School of Fudan University.

The following were purchased for the sirtuin inhibition assay and the pronase digestion  
assay, and were used as received from commercial vendors without further treatment.

Sigma-Aldrich China: the active human recombinant His<sub>6</sub>-SIRT1, Trizma, HEPES,  $\beta$ -NAD<sup>+</sup>, a

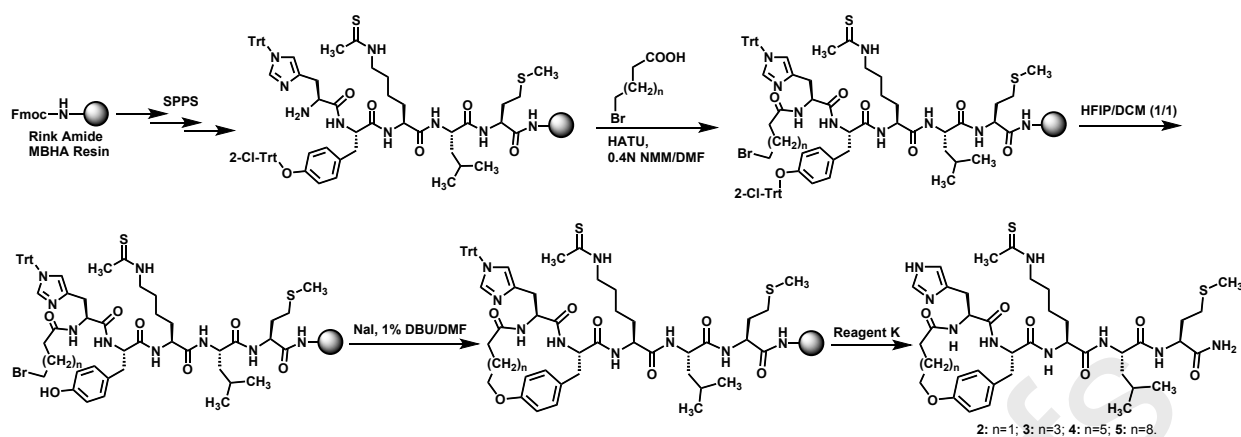
1.0 M solution of  $\text{MgCl}_2$  (molecular-biology grade), the pronase from *Streptomyces griseus*; Cayman Chemical: the active human recombinant GST-SIRT1, the active human recombinant His<sub>6</sub>-SIRT2, the active human recombinant His<sub>6</sub>-SIRT3, the active human recombinant GST-SIRT5, the active human recombinant His<sub>6</sub>-SIRT6, the active human recombinant His<sub>6</sub>-SIRT7; Thermo Fisher Scientific China: yeast tRNA (catalog #: AM7119), SUPERase-In RNase inhibitor (catalog #: AM2694); TCI Shanghai: DL-dithiothreitol (DTT); Alfa Aesar China: NaCl, KCl.

The following are the substrate peptides prepared and used in the sirtuin inhibition assay: the SIRT1/2/3 substrate  $\text{H}_2\text{N-HK-[N}^\epsilon\text{-acetyl-lysine]-LM-COOH}$  that corresponds to amino acids 380-384 of the K382-acetylated human tumor suppressor protein p53; the SIRT5 substrate  $\text{CH}_3\text{CONH-AR-[N}^\epsilon\text{-succinyl-lysine]-ST-CONH}_2$  that corresponds to amino acids 7-11 of the K9-succinylated human histone protein H3; the SIRT6 substrate  $\text{H}_2\text{N-EALPK-[N}^\epsilon\text{-myristoyl-lysine]-TGGPQ-CONH}_2$  that corresponds to amino acids 15-25 of the K20-myristoylated human tumor necrosis factor  $\alpha$  ( $\text{TNF}\alpha$ ); the SIRT7 substrate  $\text{H}_2\text{N-GGKAPR-[N}^\epsilon\text{-acetyl-lysine]-QLATKA-CONH}_2$  that corresponds to amino acids 12-24 of the K18-acetylated human histone protein H3.

## 2.2. Compound preparation

### 2.2.1. Preparation of monocyclic pentapeptides 2-5 (Scheme 1)

These compounds were synthesized by the Fmoc chemistry-based manual solid phase peptide synthesis (SPPS) on the Rink amide MBHA resin. For each amino acid coupling reaction, 4 (or 2) equiv. of a  $\text{N}^\alpha$ -Fmoc-protected amino acid, 3.8 (or 2) equiv. of the coupling



**Scheme 1.** The synthetic scheme of the monocyclic analogs **2-5**. Reagent K, a TFA-containing peptide cleavage cocktail.

reagent HBTU and the additive HOBt were used in the presence of 0.4 N NMM/DMF, and the coupling reaction was allowed to proceed at room temperature for 1 h (or 2 h). A 2% (v/v) DBU/DMF solution was used for Fmoc removal (2 x 5 min at room temperature)<sup>37</sup>. Following the on-resin assembly and the N-terminal Fmoc removal of the linear pentapeptide composed of His(Trt), Tyr(2-Cl-Trt), N<sup>ε</sup>-thioacetyl-lysine, Leu, and Met, the N-term  $\alpha$ -amino group was acylated with a bromoalkanoic acid (4-bromobutyric acid (n=1), 6-bromohexanoic acid (n=3), 8-bromooctanoic acid (n=5), or 11-bromoundecanoic acid (n=8)) (4 equiv.) in the presence of HATU (3.8 equiv.) and 0.4 N NMM/DMF (2 x 1 h at room temperature). The side chain 2-Cl-Trt protecting group of Tyr(2-Cl-Trt) was then selectively removed with 50% (v/v) HFIP/DCM (10 min at room temperature), and the exposed free side chain phenolic group was subsequently allowed to react intramolecularly with the N-term bromide in the presence of NaI (2 equiv.) and 1% (v/v) DBU/DMF (24 h at room temperature). The resulting peptidyl-resin was then treated with reagent K (83.6% (v/v) TFA, 5.9% (v/v) phenol, 4.2% (v/v) ddH<sub>2</sub>O, 4.2% (v/v) thioanisole, 2.1% (v/v) ethanedithiol) at room temperature for 4 h, followed by the filtration of the reaction mixture and the removal of the volatiles in the filtrate

with a stream of nitrogen gas in a well-ventilated fuming hood. To the resulting residue was added cold diethyl ether to precipitate out the crude pentapeptides **2-5** which were each purified with semi-preparative reversed-phase high performance liquid chromatography (RP-HPLC) on a C18 column (1 x 25 cm, 5  $\mu$ m) eluted with a gradient of ddH<sub>2</sub>O containing 0.05% (v/v) of TFA and acetonitrile containing 0.05% (v/v) of TFA at 4.5 mL/min and monitored at 214 nm. The desired RP-HPLC fractions were pooled and concentrated under reduced pressure on a rotary evaporator to remove volatiles and the remaining aqueous solution was lyophilized to afford the purified pentapeptides **2-5** all as puffy white solids. Of note, for a synthetic scale of 0.1 mmol, the purified **2-5** were obtained in overall yields of 3.1%, 12.8%, 9.2%, and 6.6%, respectively. The purified **2-5** were all >95% pure *per* RP-HPLC analysis on an analytical C18 column (0.46 x 25 cm, 5  $\mu$ m), and their exact masses were all confirmed with HRMS analysis (Table 1).

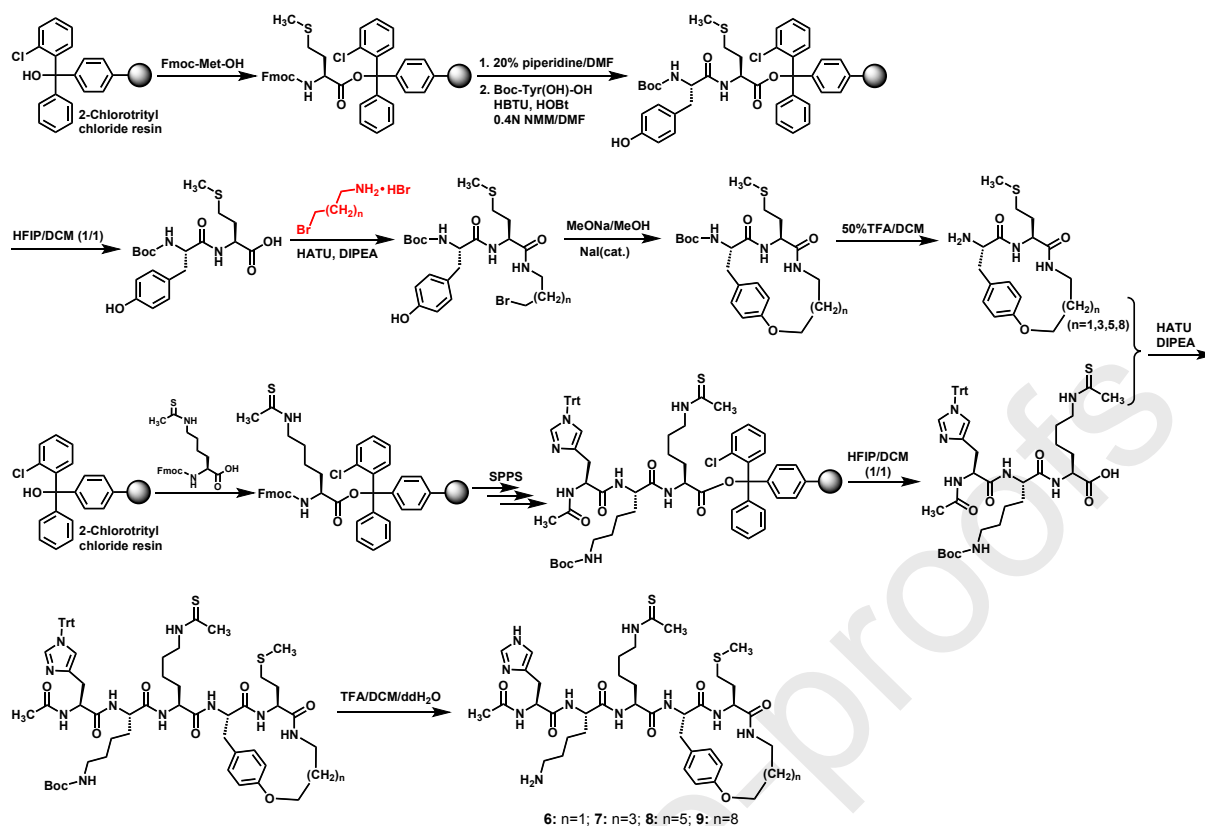
**Table 1.** The HRMS analysis of compounds **2-10**<sup>a</sup>

Compound	Ionic Formula	Calculated m/z	Observed m/z
<b>2</b>	[C <sub>38</sub> H <sub>58</sub> N <sub>9</sub> O <sub>7</sub> S <sub>2</sub> ] <sup>+</sup>	816.3895	816.3875
<b>3</b>	[C <sub>40</sub> H <sub>62</sub> N <sub>9</sub> O <sub>7</sub> S <sub>2</sub> ] <sup>+</sup>	844.4208	844.4200
<b>4</b>	[C <sub>42</sub> H <sub>66</sub> N <sub>9</sub> O <sub>7</sub> S <sub>2</sub> ] <sup>+</sup>	872.4521	872.4513
<b>5</b>	[C <sub>45</sub> H <sub>72</sub> N <sub>9</sub> O <sub>7</sub> S <sub>2</sub> ] <sup>+</sup>	914.4991	914.4981
<b>6</b>	[C <sub>39</sub> H <sub>60</sub> N <sub>10</sub> O <sub>7</sub> S <sub>2</sub> Na] <sup>+</sup>	867.3980	867.3989
<b>7</b>	[C <sub>41</sub> H <sub>64</sub> N <sub>10</sub> O <sub>7</sub> S <sub>2</sub> Na] <sup>+</sup>	895.4293	895.4300
<b>8</b>	[C <sub>43</sub> H <sub>68</sub> N <sub>10</sub> O <sub>7</sub> S <sub>2</sub> Na] <sup>+</sup>	923.4606	923.4599
<b>9</b>	[C <sub>46</sub> H <sub>74</sub> N <sub>10</sub> O <sub>7</sub> S <sub>2</sub> Na] <sup>+</sup>	965.5076	965.5070
<b>10</b>	[C <sub>46</sub> H <sub>63</sub> N <sub>9</sub> O <sub>8</sub> S <sub>2</sub> Na] <sup>+</sup>	956.4133	956.4164

<sup>a</sup> All compounds were measured with the positive ion mode of electrospray ionization (ESI).

### 2.2.2. Preparation of monocyclic pentapeptides 6-9 (Scheme 2)

These compounds each resulted from the condensation between a cyclic dipeptidic amine and a side chain fully protected linear tripeptidic acid. **(a) Preparation of a cyclic dipeptidic amine:** This started with the loading of Fmoc-Met onto the 2-chlorotrityl chloride resin in the presence of DIPEA (2 equiv.) and DCM initially at 0-2 °C for 15 min and then at room temperature for 1 h, which was followed by treating the reaction mixture with DIPEA/MeOH (v/v, 1/9) at room temperature for 15 min. The reaction mixture was then filtered and washed with DMF, isopropanol, and DCM, affording the 2-chlorotrityl resin loaded with Fmoc-Met. Following the Fmoc removal on Fmoc-Met with 20% (v/v) piperidine/DMF (2 x 10 min at room temperature), the exposed free amino group was reacted at room temperature for 2 h with Boc-Tyr(OH)-OH (4 equiv.) in the presence of HBTU (3.8 equiv.), HOBt (3.8 equiv.), and 0.4N NMM/DMF. The subsequent treatment with 50% (v/v) HFIP/DCM at room temperature for 20 min liberated from the resin the dipeptidic acid which was then reacted with a bromoalkylamine hydrobromide (n=1,5: commercially available; n=3,8: synthesized as below described according to Scheme 3) (1.2 equiv.) at room temperature for 24 h in the presence of HATU (1.2 equiv.), DIPEA (3.0 equiv.), and THF, affording the bromide intermediate with a free phenolic group which was extracted into ethyl acetate from the reaction mixture that had been concentrated under reduced pressure on a rotary evaporator, dried over anhydrous Na<sub>2</sub>SO<sub>4</sub>, and concentrated under reduced pressure on a rotary evaporator. To the obtained crude intermediate was added MeONa (1.5 equiv.), NaI (0.1 equiv.), and MeOH (freshly degassed with a stream of nitrogen gas) and the reaction mixture was stirred at room temperature for 48-72 h, affording the intermediate presumably



**Scheme 2.** The synthetic scheme of the monocyclic analogs **6-9**. **Note:** While the bromoalkylamine hydrobromide (highlighted in red) with  $n=1$  (i.e. 3-bromopropylamine hydrobromide) and  $n=5$  (i.e. 7-bromoheptylamine hydrobromide) were purchased from commercial vendors, the bromoalkylamine hydrobromide with  $n=3$  (i.e. 5-bromopentylamine hydrobromide) and  $n=8$  (i.e. 10-bromodecylamine hydrobromide) were synthesized according to Scheme 3.

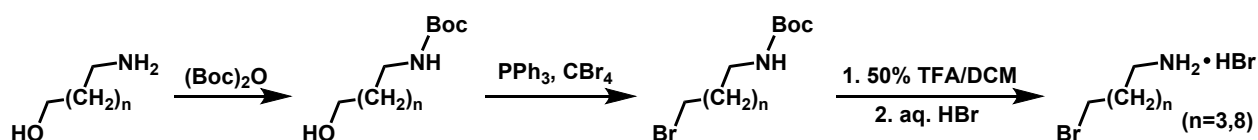
with the depicted cyclic structure which was extracted into ethyl acetate from the reaction mixture that had been concentrated under reduced pressure on a rotary evaporator, and dried over anhydrous  $\text{Na}_2\text{SO}_4$ . To the obtained crude intermediate was added 50% (v/v) TFA/DCM and the reaction mixture was stirred at room temperature for 8 h, affording the crude cyclic dipeptidic amine which was used directly for the later condensation with the side chain fully protected linear tripeptidic acid. **(b) Preparation of the side chain fully protected linear tripeptidic acid:** This started with the loading of Fmoc- $\text{N}^\epsilon$ -thioacetyl-lysine onto the 2-chlorotrityl chloride resin in the presence of DIPEA (2 equiv.) and DCM initially at 0-2 °C

for 15 min and then at room temperature for 1 h, which was followed by treating the reaction mixture with DIPEA/MeOH (v/v, 1/9) at room temperature for 15 min. The reaction mixture was then filtered and washed with DMF, isopropanol, and DCM, affording the 2-chlorotrityl resin loaded with Fmoc-N<sup>ε</sup>-thioacetyl-lysine. The sequential incorporation of Lys(Boc) and His(Trt) onto the charged 2-chlorotrityl resin was then performed based on the Fmoc chemistry-based SPPS with each amino acid coupling reaction being performed with an N<sup>α</sup>-Fmoc-protected amino acid (i.e. Fmoc-Lys(Boc)-OH or Fmoc-His(Trt)-OH) (4 equiv.), HBTU (3.8 equiv.), HOBt (3.8 equiv.) in 0.4 N NMM/DMF at room temperature for 1 h. Following the removal of the N-term Fmoc with 20% (v/v) piperidine/DMF (2 x 10 min at room temperature) and the subsequent on-resin N-term acetylation with acetic anhydride in 0.4 N NMM/DMF (1 h at room temperature), the resulting tripeptidyl resin was treated with 50% (v/v) HFIP/DCM (10 min at room temperature), affording the crude side chain fully protected linear tripeptidic acid. **(c) Preparation of monocyclic pentapeptides 6-9:** The obtained crude cyclic dipeptidic amine and the crude side chain fully protected linear tripeptidic acid were subsequently condensed in THF with HATU (1.2 equiv.) and DIPEA (1.5 equiv.) at room temperature for 24 h. The reaction mixture was then concentrated under reduced pressure on a rotary evaporator and partitioned in ddH<sub>2</sub>O and ethyl acetate. The organic layer was isolated, washed once with 5% (w/v) aqueous tartaric acid solution and once with saturated aqueous Na<sub>2</sub>CO<sub>3</sub> solution, dried over anhydrous Na<sub>2</sub>SO<sub>4</sub>, and concentrated under reduced pressure on a rotary evaporator. The obtained crude intermediate was then treated with TFA/DCM/ddH<sub>2</sub>O (90%/5%/5%, v/v/v) at room temperature for 4 h, followed by the filtration of the reaction mixture and the removal of the volatiles in the filtrate

with a stream of nitrogen gas in a well-ventilated fuming hood. To the resulting residue was added cold diethyl ether to precipitate out the crude pentapeptides **6-9** which were each purified with semi-preparative RP-HPLC on a C18 column (1 x 25 cm, 5  $\mu$ m) eluted with a gradient of ddH<sub>2</sub>O containing 0.05% (v/v) of TFA and acetonitrile containing 0.05% (v/v) of TFA at 4.5 mL/min and monitored at 214 nm. The pooled desired RP-HPLC fractions were concentrated under reduced pressure on a rotary evaporator and the remaining aqueous solution was lyophilized to afford the purified pentapeptides **6-9** all as puffy white solids. Of note, for a synthetic scale of 0.1 mmol, the purified **6-9** were obtained in overall yields of 2.4%, 6.9%, 6.7%, and 8.5%, respectively. The purified **6-9** were all >95% pure *per* RP-HPLC analysis on an analytical C18 column (0.46 x 25 cm, 5  $\mu$ m), and their exact masses were all confirmed with HRMS analysis (Table 1).

### **2.2.3. Preparation of 5-bromopentylamine hydrobromide (n=3) and 10-bromodecylamine hydrobromide (n=8) (Scheme 3)**

(a) A solution of 5-hydroxypentylamine (or 10-hydroxydecylamine) (1.0 mmol) and (Boc)<sub>2</sub>O (1.2 mmol) in dry DCM (10 mL) was stirred at room temperature for 2 h before the reaction mixture was partitioned in ddH<sub>2</sub>O (20 mL) and DCM (20 mL), the DCM layer was isolated and the ddH<sub>2</sub>O layer was extracted with DCM for three times. The combined organics were then sequentially washed with saturated aqueous NaHCO<sub>3</sub> solution and brine, dried over anhydrous Na<sub>2</sub>SO<sub>4</sub>, filtered, and concentrated under reduced pressure on a rotary evaporator. (b) To the obtained colorless oily residue was added CBr<sub>4</sub> (1.2 mmol) and dry DCM (10 mL), and the resulting solution was stirred at 0 °C while to which a solution of PPh<sub>3</sub>

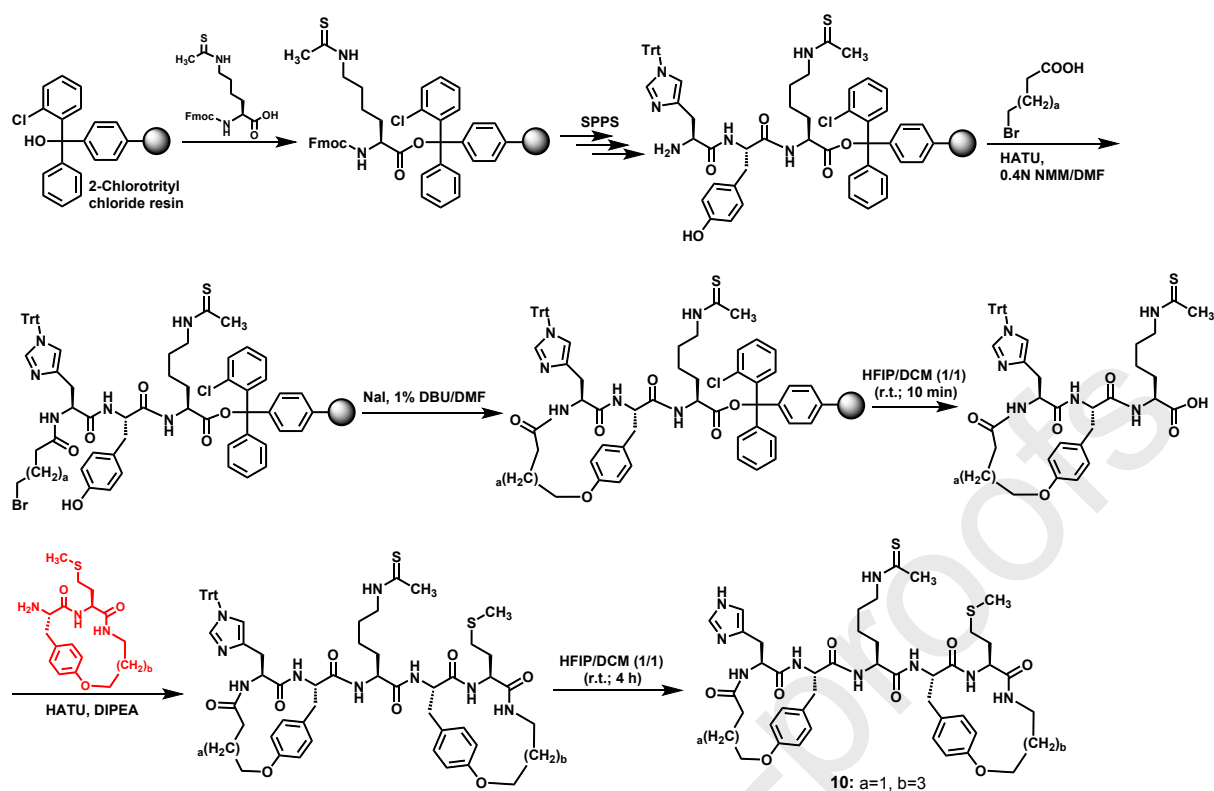


**Scheme 3.** The synthetic scheme of 5-bromopentylamine hydrobromide ( $n=3$ ) and 10-bromodecylamine hydrobromide ( $n=8$ ).

(1.2 mmol) in dry DCM (5 mL) was added. After the addition was complete, the reaction mixture was stirred at room temperature overnight before being concentrated under reduced pressure on a rotary evaporator. To the residue was then added hexanes (30 mL) while stirring, the resulting precipitate was filtered off and the filtrate was concentrated under reduced pressure again, the resulting white crystalline precipitate was filtered off again and the filtrate was then concentrated under reduced pressure. (c) To the residue (a white solid) was added 50% (v/v) TFA/DCM (6 mL) and the resulting solution was stirred at room temperature for 8 h before being concentrated. The resulting residue was then dissolved in cold diethyl ether (6 mL), and to the stirred solution was added hydrobromic acid ( $\cong 40\%$ ) ( $\sim 1.0$  mmol). The resulting white precipitate was collected *via* filtration and washed with cold diethyl ether, affording the crude material that predominantly contained 5-bromopentylamine hydrobromide (or 10-bromodecylamine hydrobromide). 5-bromopentylamine hydrobromide:  $^1\text{H}$  NMR (400 MHz,  $\text{CD}_3\text{OD}$ )  $\delta$  3.50 (t,  $J = 8.0$  Hz, 2H), 2.96 (t,  $J = 8.0$  Hz, 2H), 1.97-1.89 (m, 2H), 1.75-1.67 (m, 2H), 1.61-1.53 (m, 2H); ESI-MS calcd for  $\text{C}_5\text{H}_{13}\text{BrN}$  ( $[\text{M}+\text{H}]^+$ ) 166.02; found: 166.03. 10-bromodecylamine hydrobromide:  $^1\text{H}$  NMR (400 MHz,  $\text{CD}_3\text{OD}$ )  $\delta$  3.46 (t,  $J = 8.0$  Hz, 2H), 2.93 (t,  $J = 8.0$  Hz, 2H), 1.89-1.82 (m, 2H), 1.71-1.64 (m, 2H), 1.49-1.37 (m, 12H); ESI-MS calcd for  $\text{C}_{10}\text{H}_{23}\text{BrN}$  ( $[\text{M}+\text{H}]^+$ ) 236.10; found: 236.23. The two crude preparations were then used directly for the synthesis depicted in Scheme 2.

#### 2.2.4. Preparation of bicyclic pentapeptide 10 (Scheme 4)

This compound resulted from the condensation between the cyclic dipeptidic amine and the side chain fully protected cyclic tripeptidic acid. **(a) Preparation of the cyclic dipeptidic amine:** This particular cyclic dipeptidic amine ( $b=3$ ) was synthesized as above-described according to Scheme 2. The obtained crude material was used directly for the condensation with the crude side chain fully protected cyclic tripeptidic acid whose preparation is detailed below. **(b) Preparation of the side chain fully protected cyclic tripeptidic acid:** This started with the loading of Fmoc-N<sup>ε</sup>-thioacetyl-lysine onto the 2-chlorotrityl chloride resin in the presence of DIPEA (2 equiv.) and DCM initially at 0-2 °C for 15 min and then at room temperature for 1 h, which was followed by treating the reaction mixture with DIPEA/MeOH (v/v, 1/9) at room temperature for 15 min. The reaction mixture was then filtered and washed with DMF, isopropanol, and DCM, affording the 2-chlorotrityl resin loaded with Fmoc-N<sup>ε</sup>-thioacetyl-lysine. The subsequent sequential incorporation of Tyr(OH) and His(Trt) onto the charged 2-chlorotrityl resin was performed based on the Fmoc chemistry-based SPPS. Specifically, while Tyr(OH) was introduced with 2 equiv. of both Fmoc-Tyr(OH)-OH and HATU in 0.4 N NMM/DMF at room temperature for 2 h, the introduction of His(Trt) was realized with 4 equiv. of Fmoc-His(Trt)-OH and 3.8 equiv. of both HBTU and HOBT in 0.4 N NMM/DMF at room temperature for 1 h. The N-term N<sup>α</sup>-Fmoc removal with 20% (v/v) piperidine/DMF (2 x 10 min at room temperature) afforded the peptidyl resin with the free N-term N<sup>α</sup>-amino group and the free side chain phenolic group of Tyr(OH). The N-term α-amino group was then selectively acylated with 4-bromobutyric acid ( $a=1$ ) (4 equiv.) in the presence of HATU (3.8 equiv.) and 0.4 N NMM/DMF (2 x 1 h at room temperature). The free



**Scheme 4.** The synthetic scheme of the bicyclic analog **10**. **Note:** The cyclic dipeptidic amine ( $b=3$ ) whose chemical structure is highlighted in red was synthesized as depicted in Scheme 2.

side chain phenolic group of Tyr(OH) was subsequently allowed to react intramolecularly with the N-term bromide in the presence of Trt NaI (2 equiv.) and 1% (v/v) DBU/DMF (2 x 36 h at room temperature). The final treatment with 50% (v/v) HFIP/DCM at room temperature for 10 min afforded the crude side chain fully protected cyclic tripeptidic acid. **(c) Preparation of bicyclic pentapeptide 10:** The obtained crude cyclic dipeptidic amine and side chain fully protected cyclic tripeptidic acid were subsequently condensed in THF with HATU (1.2 equiv.) and DIPEA (1.5 equiv.) at room temperature for 24 h. The reaction mixture was then concentrated under reduced pressure on a rotary evaporator and the obtained residue was taken into ethyl acetate. The organic layer was washed once with 5% (w/v) aqueous tartaric acid solution and once with saturated aqueous  $\text{Na}_2\text{CO}_3$  solution, and dried over anhydrous

Na<sub>2</sub>SO<sub>4</sub>. After filtration, the filtrate was concentrated under reduced pressure on a rotary evaporator, and the obtained residue was then treated with 50% (v/v) HFIP/DCM at room temperature for 4 h followed by the removal of the volatiles in the reaction mixture under reduced pressure on a rotary evaporator. To the resulting residue was added cold diethyl ether to precipitate out the crude pentapeptide **10** which was purified with semi-preparative RP-HPLC on a C18 column (1 x 25 cm, 5 μm) eluted with a gradient of ddH<sub>2</sub>O containing 0.05% (v/v) of TFA and acetonitrile containing 0.05% (v/v) of TFA at 4.5 mL/min and monitored at 214 nm. The pooled desired RP-HPLC fractions were concentrated under reduced pressure on a rotary evaporator and the remaining aqueous solution was lyophilized to afford the purified pentapeptide **10** as a puffy white solid. Of note, for a synthetic scale of 0.1 mmol, the purified **10** was obtained in an overall yield of 1.4%. The purified **10** was >95% pure *per* RP-HPLC analysis on an analytical C18 column (0.46 x 25 cm, 5 μm), and its exact mass was confirmed with HRMS analysis (Table 1).

### 2.3. *In vitro* sirtuin inhibition assay with compounds 2-10

The HPLC-based sirtuin inhibition assay was employed in the current study and was performed as described previously<sup>38-40</sup>. An assay solution (50 μL) contained the following components: 50 mM Hepes (pH 8.0), 137 mM NaCl (150 mM for the SIRT7 assay), 2.7 mM KCl and 1 mM MgCl<sub>2</sub> (both omitted for the SIRT7 assay), 1 mM DTT, yeast tRNA (3-fold molar excess relative to SIRT7) and SUPERase-In RNase inhibitor (to a final concentration of ~1 U/μL, to inhibit tRNA degradation) (both for the SIRT7 assay only), β-NAD<sup>+</sup> (0.5 mM for the SIRT1 and SIRT2 assays, 3.5 mM for the SIRT3 assay, 0.8 mM for the SIRT5 assay, 0.2

mM for the SIRT6 assay, or 3 mM for the SIRT7 assay), the peptide substrate (0.3 mM of the above-mentioned SIRT1/2/3 acetyl-lysine substrate for the SIRT1 assay, 0.39 mM of the above-mentioned SIRT1/2/3 acetyl-lysine substrate for the SIRT2 assay, 0.105 mM of the above-mentioned SIRT1/2/3 acetyl-lysine substrate for the SIRT3 assay, 0.88 mM of the above-mentioned SIRT5 succinyl-lysine substrate, 0.02 mM of the above-mentioned SIRT6 myristoyl-lysine substrate, or 1.8 mM of the above-mentioned SIRT7 acetyl-lysine substrate), one test compound (purified **2-10**) with varied concentrations including 0, and a sirtuin (His<sub>6</sub>-SIRT1 or GST-SIRT1, 320 nM; His<sub>6</sub>-SIRT2, 309 nM; His<sub>6</sub>-SIRT3, 320 nM; GST-SIRT5, 370 nM; His<sub>6</sub>-SIRT6, 313 nM; or His<sub>6</sub>-SIRT7, 570 nM). The same [S]/K<sub>m</sub> ratios for both substrates (~3.2 for the peptide substrates and ~5.6 for β-NAD<sup>+</sup>) were employed for the inhibition assays with all the six human sirtuins (SIRT1/2/3/5/6/7) employed in the current study. An enzymatic reaction was initiated by the addition of a sirtuin at 37 °C and was allowed to be incubated at 37 °C for 10 min (for the SIRT1 assay), 12 min (for the SIRT2 assay), 10 min (for the SIRT3 assay), 5 min (for the SIRT5 assay), 12 min (for the SIRT6 assay), or 30 min (for the SIRT7 assay) until quenched with the following stop solution: 100 mM HCl and 0.16 M acetic acid. The quenched assay solutions were directly injected into a reversed-phase C18 column (0.46 x 25 cm, 5 μm) eluted with a gradient of ddH<sub>2</sub>O containing 0.05% (v/v) TFA and acetonitrile containing 0.05% (v/v) TFA at 1 mL/min and monitored at 214 nm. Turnover of the limiting substrate was maintained at < 10%. Stock solutions of the test compounds were all prepared in ddH<sub>2</sub>O. IC<sub>50</sub> values were estimated from the Dixon plots (1/v<sub>0</sub> vs. [inhibitor])<sup>41</sup> as an indication of the inhibitory potency.

#### 2.4. Pronase digestion assay with compounds **1** and **10**

This assay was also performed as described previously<sup>39</sup>. Fifty (50)  $\mu\text{L}$  of a solution of a test compound (**1** or **10**) in ddH<sub>2</sub>O (160  $\mu\text{M}$ ) was mixed thoroughly with 50  $\mu\text{L}$  of a pronase solution in 100 mM Tris•HCl (pH 7.3) (8 ng/ $\mu\text{L}$ ), and the resulting solution was incubated at 37 °C until quenched with a 1.0 M solution of acetic acid in ddH<sub>2</sub>O at 0, 1, and 2 min for **1** or at 0, 2.5, 5.0, 10, 20, and 30 min for **10**. At each time point, 20  $\mu\text{L}$  of a pronase digestion mixture was taken and treated with 40  $\mu\text{L}$  of the 1.0 M acetic acid solution, and the whole mixture was vigorously vortexed, centrifuged, and the supernatant was injected into a reversed-phase C18 analytical HPLC column (0.46 x 25 cm, 5  $\mu\text{m}$ ). The C18 column was eluted with a gradient of ddH<sub>2</sub>O containing 0.05% (v/v) TFA and acetonitrile containing 0.05% (v/v) TFA at 1 mL/min and monitored at 214 nm. The HPLC peak areas obtained for a given test compound at different time points were used to estimate the percentage remaining for this test compound with the digestion time. The graph of the percentage remaining *versus* time was used to compare the proteolytic stability of different test compounds, as shown in Fig. 3.

#### 2.5. Western blotting analysis with compound **10**

This assay was also performed as previously described by Zheng laboratory<sup>35,39</sup>. Briefly, HCT116 human colon cancer cells (Procell, Wuhan, China) ( $5 \times 10^5$ ) were cultured in McCoy5A culture medium containing 10% FBS and were treated for 8 h at 37 °C with compound **10** (stock solution prepared in ddH<sub>2</sub>O) at different final concentrations (0, 0.5, 2, 10, 50, and 100  $\mu\text{M}$ ) before cell lysis and SDS-PAGE. Proteins on a SDS-PAGE gel were then transferred onto a PVDF membrane (Millipore). The transblotted membrane was blocked

for 2 h at room temperature and then incubated overnight at 4 °C with the following primary antibodies: acetyl-p53 (K382) antibody (Cell Signaling Technology, United States) and p53 antibody (Proteintech-CN, Wuhan, China). After the treatment with the above primary antibodies, the transblotted membrane was treated with the goat anti-rabbit IgG (H+L) secondary antibody-horseradish peroxidase (HRP) conjugate (Boster (PRC), Wuhan, China) for 2 h at 37 °C, and the immunoblots (for K382-acetylated p53 protein and total p53 protein) were visualized by enhanced chemiluminescence.

## 2.6. Cell proliferation assay with compound **10**

This assay was performed as previously described by George et al. on the anti-proliferative effect of 4'-bromo-resveratrol on melanoma cells<sup>42</sup>. Of note, 4'-bromo-resveratrol was found earlier by Nguyen et al. to be a potent inhibitor against the deacetylase activity of human SIRT1 and SIRT3 under the assay condition of the study<sup>43</sup>. The human MCF-7 breast cancer cells (Procell, Wuhan, China) and the human SK-MEL-2 melanoma cells (Beijing zhongkezhijian Biotechnology Co. Ltd., Beijing, China) were employed in our current study, and the anti-proliferative effect of compound **10** was assessed with the 3-(4,5-dimethylthiazol-2-yl)-2,5-diphenyltetrazolium bromide (MTT)-based assay. Briefly, MCF-7 cells ( $5 \times 10^3$ , 100  $\mu$ L cell suspension) or SK-MEL-2 cells ( $5 \times 10^3$ , 100  $\mu$ L cell suspension) were cultured in 96-well plates in DMEM culture medium containing 10 % FBS (for MCF-7 cells) or MEM culture medium containing 10% FBS (for SK-MEL-2 cells) overnight and then were treated at 37 °C with compound **10** (stock solution prepared in ddH<sub>2</sub>O) at different final concentrations (0, 5, 12.5, 25, 50, or 100  $\mu$ M) for 24 h, 48 h, or 72 h.

The cells in each treatment well were then washed with phosphate buffered saline (PBS) and subsequently incubated with 10  $\mu$ L of a 5 mg/mL solution of MTT in PBS (to a final concentration of 0.5 mg/mL) at 37 °C for 4 h. After the removal of the incubation buffer by pipetting, to each treatment well was then added 150  $\mu$ L of DMSO, and the resulting mixture was agitated for 10 min before the absorbance at 568 nm was measured for each treatment well. The assay results are presented in Fig. 5.

### 3. Results and Discussion

#### 3.1. Compound design

Fig. 2 depicts the monocyclic and bicyclic pentapeptides **2-10** we prepared in the current study which are the analogs of the linear pentapeptide-based potent (sub- $\mu$ M IC<sub>50</sub>'s) pan-SIRT1/2/3 inhibitor **1** Zheng laboratory discovered recently<sup>44</sup> that harbors the catalytic mechanism-based SIRT1/2/3 inhibitory warhead N<sup>ε</sup>-thioacetyl-lysine (discovered during 2006-2007 by Zheng laboratory<sup>36</sup> and that of Denu<sup>45</sup>) at its central position. Despite being a potent pan-SIRT1/2/3 inhibitor, the linear peptide **1** could be less proteolytically stable and cell permeable than its cyclic analogs because peptide chain cyclization is known to be able to potentially enhance the proteolytic stability and the cell permeability of a parent linear peptide<sup>46</sup>. To pursue the cyclic analogs of **1**, we initially designed and prepared four monocyclic analogs with N-term macrocycles and four monocyclic analogs with C-term macrocycles depicted in Fig. 2, hoping to find the N-term and the C-term macrocycles able to confer stronger SIRT1/2/3 inhibition than **1** so that these macrocycles could be employed to

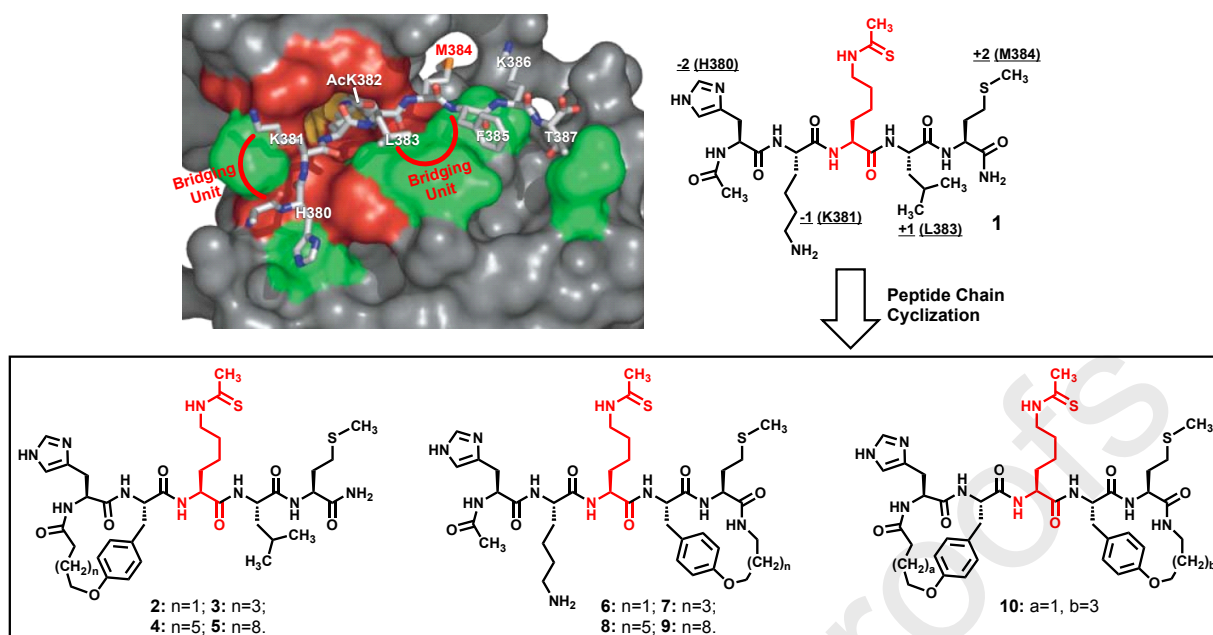


**Fig. 2.** The design of the monocyclic analogs **2-9** and the bicyclic analog **10** of the linear pentapeptide **1** *via* peptide chain cyclization. **Note:** (i) The central N<sup>ε</sup>-thioacetyl-lysine residue (highlighted in red) of **1** corresponds to the N<sup>ε</sup>-acetyl-lysine residue (AcK382) of the peptide substrate that is depicted to be bound at the active site of archaeal Sir2-Af2 in the upper left 3-dimensional rendering (adapted from ref. 47 with permission) of the X-ray crystallographically determined structure of the complex of Sir2-Af2 and the depicted peptide substrate (Protein Data Bank code: 1MA3). (ii) The side chains at the -2, -1, +1, and +2 positions of **1** respectively correspond to the H380, K381, L383, and M384 residues of the bound peptide substrate depicted in the upper left 3-dimensional rendering. (iii) The red, yellow, and green regions in the upper left 3-dimensional rendering refer to the degree of amino acid conservation (conserved, similar, and variable, respectively) among the following ten sirtuins based on sequence alignment: Sir2-Af1, Sir2-Af2, Sir2-Tm, Sir2, Hst1, Hst2, CobB, SIRT1, SIRT2, and SIRT5. (iv) The two thick red curves in the upper left depiction refer to the macrocycle bridging units present in cyclic analogs **2-10**.

construct bicyclic analogs, which was pursued because the other half of the molecule of a monocyclic analog is still a proteolytically labile linear peptide harboring two consecutive standard amino acids.

The monocyclic analogs **2-9** were designed based on the following: (i) the substrate recognition behavior at a sirtuin active site would be applicable to a N<sup>ε</sup>-thioacetyl-lysine-containing catalytic mechanism-based sirtuin inhibitor since such an

inhibitor would be first recognized and processed as a sirtuin substrate, however with the formation of a sirtuin inhibiting species latter on along the catalytic coordinate<sup>8,32,48</sup>; (ii) N<sup>ε</sup>-acetyl-lysine and its four immediately flanking amino acid residues (two on each side) in a substrate form a  $\beta$ -strand in a sirtuin bound substrate and this  $\beta$ -strand forms an anti-parallel  $\beta$ -sheet with two  $\beta$ -strands from a sirtuin active site, as first observed in the X-ray co-crystal structure of archaeal Sir2-Af2 complexed with the substrate peptide depicted in Fig. 2<sup>47</sup>; (iii) the tyrosine replacement for the native amino acid residues at -1 and +1 positions relative to N<sup>ε</sup>-thioacetyl-lysine was previously demonstrated by Zheng laboratory to be tolerable concerning the SIRT1 inhibitory potency with the sequence of HK-(N<sup>ε</sup>-thioacetyl-lysine)-LM<sup>39</sup>; (iv) the N-term and the C-term macrocycles in the monocyclic pentapeptides **2-9** are or closely resemble those that have been demonstrated previously by Fairlie and co-workers to be effective local  $\beta$ -strand inducers in a peptide sequence<sup>49,50</sup>. In addition, according to the 3-dimensional rendering depicted in Fig. 2, the N-term and C-term macrocycle units in pentapeptides **2-9** would have a favorable global fit at sirtuin active site.

### 3.2. Compound preparation

The monocyclic pentapeptides **2-5** with N-term macrocycle units were synthesized according to Scheme 1. The linear pentapeptide composed of His(Trt), Tyr(2-Cl-Trt), N<sup>ε</sup>-thioacetyl-lysine, Leu, and Met was initially assembled on the Rink amide MBHA resin based on the Fmoc chemistry-based manual SPPS followed by the N-term N<sup>α</sup>-Fmoc removal, the N-term free  $\alpha$ -amino group was then acylated with a bromoalkanoic acid (4-bromobutyric

acid (n=1), 6-bromohexanoic acid (n=3), 8-bromooctanoic acid (n=5), or 11-bromoundecanoic acid (n=8)) in the presence of HATU and 0.4 N NMM/DMF. The side chain 2-Cl-Trt protecting group of Tyr(2-Cl-Trt) was then selectively removed with 50% (v/v) HFIP/DCM, and the exposed free side chain phenolic group was subsequently allowed to react intra-molecularly with the N-term bromide in the presence of NaI and 1% (v/v) DBU/DMF. The final treatment of the resulting peptidyl-resin with Reagent K (a TFA-containing peptide cleavage cocktail) afforded the crude pentapeptides **2-5** which were each purified by semi-preparative RP-HPLC. The exact masses of the purified **2-5** were confirmed by HRMS analysis (Table 1). The purified **2-5** were each >95% pure based on a RP-HPLC analysis.

The monocyclic pentapeptides **6-9** with C-term macrocycle units were synthesized according to Scheme 2. As depicted, these compounds each resulted from the condensation between a cyclic dipeptidic amine and a side chain fully protected linear tripeptidic acid. The synthesis of a cyclic dipeptidic amine started with the loading of Fmoc-Met onto the 2-chlorotrityl chloride resin, followed by Fmoc removal and the subsequent coupling with Boc-Tyr-OH. Following treating the resulting dipeptidyl resin with 50% (v/v) HFIP/DCM, the dipeptidic acid cleaved from the resin was reacted in solution with a bromoalkylamine hydrobromide (3-bromopropylamine hydrobromide (n=1), 5-bromopentylamine hydrobromide (n=3), 7-bromoheptylamine hydrobromide (n=5), or 10-bromodecylamine hydrobromide (n=8)). The phenolic group and the bromide in the resulting intermediate were then allowed to undergo an intra-molecular cyclization in the presence of MeONa and NaI. The final treatment with 50% (v/v) TFA/DCM afforded the crude cyclic dipeptidic amine

which was used directly for the later condensation with the side chain fully protected linear tripeptidic acid, whose synthesis is detailed below starting with the loading of Fmoc-N<sup>ε</sup>-thioacetyl-lysine onto the 2-chlorotrityl chloride resin. The sequential incorporation of Lys(Boc) and His(Trt) onto the charged 2-chlorotrityl resin based on the Fmoc chemistry-based SPPS followed by the N-terminal N<sup>α</sup>-acetylation with acetic anhydride afforded the side chain fully protected linear tripeptidyl resin. The final treatment with 50% (v/v) HFIP/DCM afforded the crude side chain fully protected linear tripeptidic acid which was used directly for the condensation with the above-described crude cyclic dipeptidic amine in solution, and the resulting intermediate was then treated with a TFA-containing peptide cleavage cocktail, affording the crude pentapeptides **6-9** which were each also purified by semi-preparative RP-HPLC. The exact masses of the purified **6-9** were also confirmed by HRMS analysis (Table 1). The purified **6-9** were each also >95% pure based on a RP-HPLC analysis.

The bicyclic pentapeptide **10** was synthesized according to Scheme 4. As depicted, this compound resulted from the condensation between the cyclic dipeptidic amine and the side chain fully protected cyclic tripeptidic acid. The synthesis of the side chain fully protected cyclic tripeptidic acid started with the loading of Fmoc-N<sup>ε</sup>-thioacetyl-lysine onto the 2-chlorotrityl chloride resin. The subsequent sequential incorporation of Tyr(OH) and His(Trt) based on the Fmoc chemistry-based SPPS followed by the N-term N<sup>α</sup>-Fmoc removal afforded the peptidyl resin with the free N-term N<sup>α</sup>-amino group and the free side chain phenolic group of Tyr(OH). The N-term α-amino group was then selectively acylated with 4-bromobutyric acid (a=1) in the presence of HATU and 0.4 N NMM/DMF. The free side chain phenolic

group of Tyr(OH) was subsequently allowed to react intra-molecularly with the N-term bromide in the presence of NaI and 1% (v/v) DBU/DMF. The final treatment with 50% (v/v) HFIP/DCM afforded the crude side chain fully protected cyclic tripeptidic acid which was subsequently used directly for the condensation in solution with the crude cyclic dipeptidic amine (b=3) which was synthesized as above-described according to Scheme 2. The resulting intermediate was then treated with 50% (v/v) HFIP/DCM (4 h at room temperature), affording the crude bicyclic pentapeptide **10** which was also purified by semi-preparative RP-HPLC. The exact mass of the purified **10** was also confirmed by HRMS analysis (Table 1). The purified **10** was also >95% pure based on a RP-HPLC analysis.

### 3.3. *In vitro* sirtuin inhibition assay

When the purified monocyclic pentapeptides **2-9** were subjected to a HPLC-based *in vitro* sirtuin inhibition assay, we found that the SIRT1/2/3 inhibitory potencies of **2-5** (especially **2**) were much closer to those of the linear pentapeptide **1** than the SIRT1/2/3 inhibitory potencies of **6-9** (Table 2). Therefore, it is clear that, even though the tyrosine side chains at both -1 and +1 positions relative to N<sup>ε</sup>-thioacetyl-lysine in the template sequence HK-(N<sup>ε</sup>-thioacetyl-lysine)-LM could be accommodated favorably at a sirtuin active site, as previously demonstrated with SIRT1<sup>39</sup>, the engagement of the side chain phenolic group of the tyrosine residue at the +1 position as in the C-term macrocycles of **6-9** led to dramatically attenuated binding at SIRT1/2/3 active sites. While the above finding with monocyclic pentapeptides **6-9** is disappointing, their macrocycles may still have a favorable global fit (albeit with unfavorable binding details) at sirtuin active site according to the 3-dimensional

**Table 2.** SIRT1/2/3 inhibition by compounds **1-10**<sup>a</sup>

Compound	IC <sub>50</sub> (μM) <sup>b</sup>		
	SIRT1	SIRT2	SIRT3
<b>1</b> <sup>c</sup>	0.165 ± 0.048	0.332 ± 0.062	0.27 ± 0.024
<b>2</b>	0.171 ± 0.059	0.68 ± 0.3	0.75 ± 0.3
<b>3</b>	0.646 ± 0.204	1.03 ± 0.29	0.53 ± 0.16
<b>4</b>	0.673 ± 0.199	1.33 ± 0.078	0.55 ± 0.26
<b>5</b>	1.25 ± 0.57	4.31 ± 2.74	1.1 ± 0.54
<b>6</b>	34.3 ± 8.3	60.8 ± 15.6	90.9 ± 7.6
<b>7</b>	13.6 ± 1.9	115.1 ± 41.6	177.1 ± 47.4
<b>8</b>	22.6 ± 7.4	25.5 ± 0.85	217.3 ± 38.7
<b>9</b>	56.7 ± 7.4	17.9 ± 0.42	13.1 ± 3.0
<b>10</b>	0.54 ± 0.07	0.253 ± 0.02	0.72 ± 0.36

<sup>a</sup> The SIRT1/2/3-catalyzed reaction monitored in the inhibition assay was deacetylation. See “Materials and Methods” for assay detail. <sup>b</sup> IC<sub>50</sub>, the inhibitor concentration at which an enzymatic reaction velocity is reduced by 50%. <sup>c</sup> Taken from ref. 44 in which compound **1** was evaluated under identical SIRT1/2/3 inhibition assay condition to that used in the current study.

rendering depicted in Fig. 2, we were therefore interested in constructing a bicyclic pentapeptide composed of the macrocycles selected from those in the monocyclic pentapeptides **2-9**, hoping the binding of the N-term macrocycle would incur a better binding at sirtuin active site for the C-term macrocycle. Fig. 2 shows the chemical structure of the bicyclic pentapeptide (i.e. **10**) we prepared in the current study. Its N-term macrocycle corresponds to that of **2** since **2** was the most potent SIRT1/2/3 inhibitor among **2-5**; its C-term macrocycle corresponds to that of **7** since **7** exhibited the strongest SIRT1 inhibition among **6-9**.

When the purified bicyclic pentapeptide **10** was subjected to the HPLC-based *in vitro* sirtuin inhibition assay, this compound was found to exhibit a strong pan-SIRT1/2/3

inhibition. As shown in Table 2, the SIRT1/2/3 inhibitory potencies of the bicyclic pentapeptide **10** are largely comparable to those of the linear pentapeptide **1** ( $IC_{50}$  values within 3.3-fold of difference). We further found that the inhibition of **10** against the SIRT5/6/7-catalyzed deacylation reactions (i.e. desuccinylation, demyristoylation, and the tRNA-activated deacetylation, respectively) was very weak with respective  $IC_{50}$  values being  $442.7 \pm 178.9 \mu\text{M}$ ,  $390.2 \pm 23.3 \mu\text{M}$ , and  $78.9 \pm 13.9 \mu\text{M}$ , which ought to be consistent with the fact that deacetylation is a less proficient catalytic activity of SIRT5/6/7<sup>1,4,5,7,8,51</sup>.

### 3.4. Pronase digestion assay

Even though the bicyclic pentapeptide **10** was found to be a comparably strong pan-SIRT1/2/3 inhibitor to the linear pentapeptide **1**, the potential of peptide chain cyclization to enhance the proteolytic stability of a parent linear peptide<sup>46</sup> prompted us to subject the fully cyclic compound **10** and the fully linear compound **1** to a proteolysis experiment to compare their proteolytic stability. Pronase was used in the experiment as the proteolytic enzyme preparation because pronase is a mixture of different types of proteases and peptidases and thus exhibits a very broad substrate specificity<sup>52</sup>. As indicated in Fig. 3, the bicyclic pentapeptide **10** is proteolytically much more stable than the linear pentapeptide **1**. Therefore, compound **10** rather than compound **1** would be a more appropriate lead compound for further development. As such, in the current study compound **10** was evaluated further with the following preliminary studies.

### 3.5. Western blotting analysis

As revealed by such an analysis and indicated in Fig. 4, the bicyclic pentapeptide **10** was found to be cell permeable and able to inhibit the SIRT1-catalyzed deacetylation of the K382-acetylated tumor suppresser protein p53 (a native SIRT1 substrate<sup>53</sup>) inside the human HCT116 colon cancer cells, as judged by a concentration-dependent increase in the p53 acetylation at K382 following the treatment of cells with **10**.

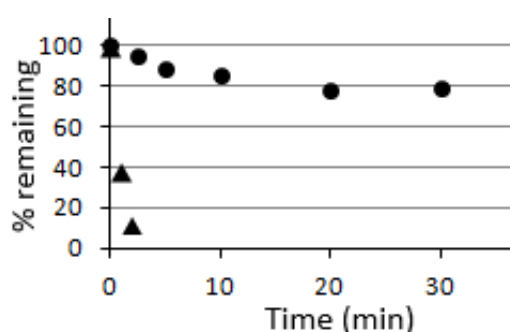


**Fig. 3.** The proteolysis profiles of compounds **10** (●) and **1** (▲). Each data point is the mean of two measurements with standard deviation less than 15%. See “Materials and Methods” for the proteolysis assay details.

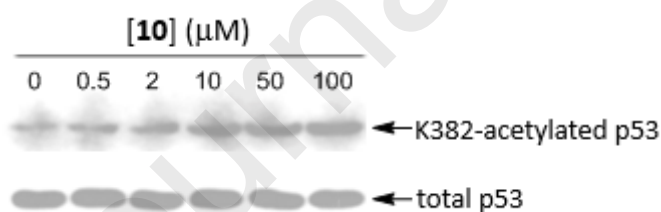


**Fig. 4.** The Western blotting analysis of the tumor suppresser protein p53 K382-acetylation level change in the human HCT116 colon cancer cells following the treatment with compound **10**. See “Materials and Methods” for the experimental details.

### 3.6. Cell proliferation assay

The human MCF-7 breast cancer cells and the human SK-MEL-2 melanoma cells were employed in this assay, and the anti-proliferative effect of compound **10** was assessed with

the MTT-based assay. The roughly comparable SIRT1/2 dual inhibition by compound **10** made us select the human MCF-7 cells for our current assay since a dual SIRT1/2 inhibition was previously demonstrated with the human MCF-7 cells to be necessary for cell growth inhibition<sup>54</sup>. Moreover, the roughly comparable SIRT1/3 dual inhibition by compound **10** made us also select the human SK-MEL-2 cells for our current assay since this type of the cells were also used previously to examine the anti-proliferative effect of 4'-bromo-resveratrol<sup>42</sup> which was found earlier to be a potent SIRT1/3 dual inhibitor under the assay condition of the study<sup>43</sup>, even though its inhibitory action on other human sirtuins (e.g. SIRT2) was not assessed in the study. As indicated in Fig. 5, while there is a general trend of increased concentration-dependent cell growth inhibition as the treatment time of compound **10** was increased (from 24 h to 48 h and to 72 h) with both types of the cells, the overall inhibitory strength of compound **10** is much greater toward the human SK-MEL-2 cells than that toward the human MCF-7 cells. This finding suggests that a SIRT1/2/3 triple inhibition seems to be more able to confer a growth inhibition against the human melanoma cells than against the human breast cancer cells. It should be noted that, under our assay condition, tamoxifen treatment at 100  $\mu$ M and 24h/48h/72h was found to be all able to confer an over 80% growth inhibition against the human MCF-7 cells (data not shown), suggesting that the observed weak inhibition of compound **10** treatment was not due to possible problems with the human MCF-7 cells used in our assay.

#### 4. Conclusion

To summarize, we found in the current study that the bicyclic analog **10** of the

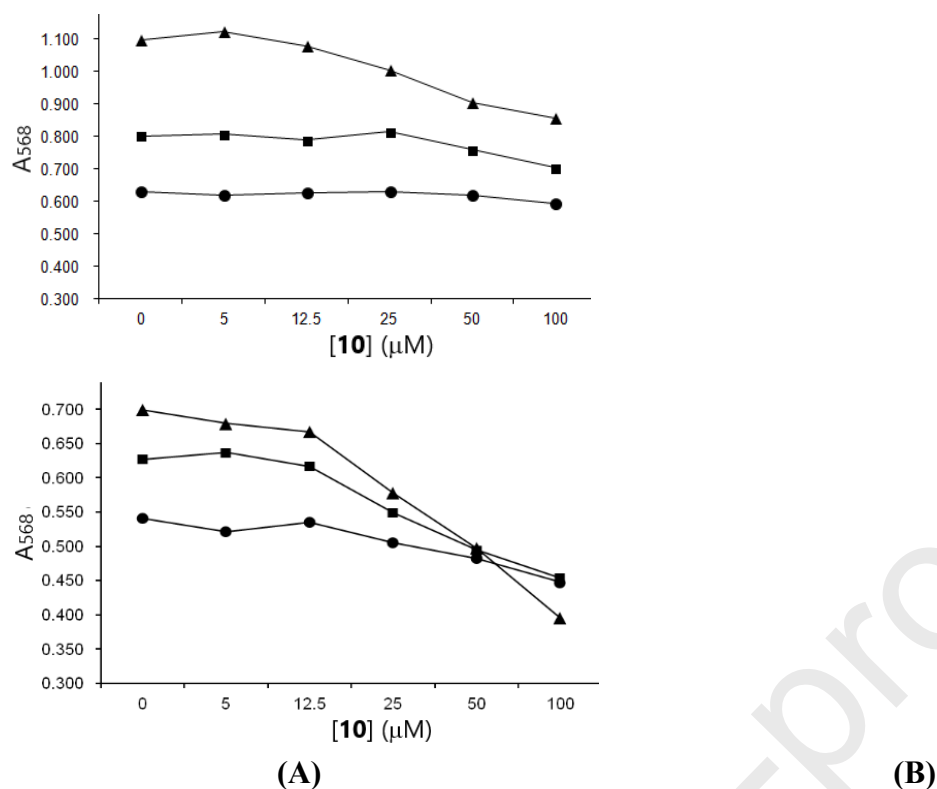


**Fig. 5.** The MTT-based assay of the anti-proliferative effect on the human MCF-7 breast cancer cells (A) and the human SK-MEL-2 melanoma cells (B) following the treatment with compound **10** for 24 h (●), 48 h (■), or 72 h (▲). Each data point is the mean of five measurements with standard deviation less than 7%. See “Materials and Methods” for the assay details.

$N^{\epsilon}$ -thioacetyl-lysine-containing linear pentapeptide-based potent pan-SIRT1/2/3 inhibitor **1** also behaved as a potent pan-SIRT1/2/3 inhibitor while additionally exhibiting very weak SIRT5/6/7 inhibition. Even though the SIRT1/2/3 inhibitory potencies of **10** are largely comparable to those of **1**, **10** was found to be proteolytically much more stable than **1**, suggesting that **10** rather than **1** would be a more appropriate lead compound for further development. Compound **10** was further found to be cell permeable and able to inhibit the SIRT1-catalyzed deacetylation inside the human HCT116 colon cancer cells. Moreover, the preliminary cell proliferation assay revealed that compound **10** was able to inhibit the growth of the human SK-MEL-2 melanoma cells to a much greater extent than that of the human

MCF-7 breast cancer cells. It should be noted that several thieno[3,2-d]pyrimidine-6-carboxamides derived from a small molecule library screening were reported in 2013 by Disch et al. to be fairly strong pan-SIRT1/2/3 inhibitors with the most notable example exhibiting inhibitory IC<sub>50</sub> values of 4.3 nM, 1.1 nM, and 7.2 nM against SIRT1, SIRT2, and SIRT3, respectively, under the assay condition of the study<sup>55</sup>. However, the inhibitory potencies of the compounds reported by Disch et al. against human sirtuins other than SIRT1/2/3 (like SIRT5/6/7) and thus the pan-SIRT1/2/3 inhibitory selectivity are unknown, and given that their compounds were of a novel chemotype, such inhibitory potencies and selectivity are difficult to predict. Therefore, bicyclic pentapeptide **10** identified in our current study represents the first highly potent and selective pan-SIRT1/2/3 inhibitor ever identified; and the additional characterization of this compound in our current study suggests that it could be an appropriate lead compound for the future development of more potent yet still selective pan-SIRT1/2/3 inhibitors whose use in the studies on human sirtuin biology, pharmacology, and medicinal chemistry could complement with the use of the potent inhibitors selective for a single human sirtuin.

### **Acknowledgements**

The following are highly appreciated for the financial support to this work: the National Natural Science Foundation of China (grant no. 21272094), the Jiangsu provincial specially appointed professorship, and the Jiangsu provincial “innovation and venture talents” award plan.

### **Competing interests**

The authors declare no competing interests.

## Supplementary information

Copies of the RP-HPLC traces for the purified cyclic peptides **2-10**.

## References

1. Ringel, A. E.; Tucker, S. A.; Haigis, M. C. Chemical and physiological features of mitochondrial acylation. *Mol. Cell* **2018**, *72*, 610-624.
2. Li, Y.; Zhou, Y.; Wang, F.; Chen, X.; Wang, C.; Wang, J.; Liu, T.; Li, Y.; He, B. SIRT4 is the last puzzle of mitochondrial sirtuins. *Bioorg. Med. Chem.* **2018**, *26*, 3861-3865.
3. Hu, X.; Zheng, W. Chemical probes in sirtuin research. In *Progress in Molecular Biology and Translational Science. Sirtuins in Health and Disease*; 1st ed.; Zheng, W., Ed.; Academic Press: Cambridge, MA, USA, 2018; Volume 154, pp. 1-24.
4. Rajabi, N.; Galleano, I.; Madsen, A.S.; Olsen, C.A. Targeting sirtuins: Substrate specificity and inhibitor design. In *Progress in Molecular Biology and Translational Science. Sirtuins in Health and Disease*; 1st ed.; Zheng, W., Ed.; Academic Press: Cambridge, MA, USA, 2018; Volume 154, pp. 25-69.
5. Li, S.; Zheng, W. Mammalian sirtuins SIRT4 and SIRT7. In *Progress in Molecular Biology and Translational Science. Sirtuins in Health and Disease*; 1st ed.; Zheng, W., Ed.; Academic Press: Cambridge, MA, USA, 2018; Volume 154, pp. 147-168.
6. Carabetta, V. J.; Cristea, I. M. Regulation, function, and detection of protein acetylation in bacteria. *J. Bacteriol.* **2017**, *199*, pii: e00107-17.
7. Bheda, P.; Jing, H.; Wolberger, C.; Lin, H. The substrate specificity of sirtuins. *Annu. Rev.*

*Biochem.* **2016**, *85*, 405-429.

8. Chen, B.; Zang, W.; Wang, J.; Huang, Y.; He, Y.; Yan, L.; Liu, J.; Zheng, W. The chemical biology of sirtuins. *Chem. Soc. Rev.* **2015**, *44*, 5246-5264.

9. Martínez-Redondo, P.; Vaquero, A. The diversity of histone versus nonhistone sirtuin substrates. *Genes Cancer* **2013**, *4*, 148-163.

10. Wagner, G. R.; Hirschey, M. D. Nonenzymatic protein acylation as a carbon stress regulated by sirtuin deacylases. *Mol. Cell* **2014**, *54*, 5-16.

11. Carrico, C.; Meyer, J. G.; He, W.; Gibson, B. W.; Verdin, E. The mitochondrial acylome emerges: proteomics, regulation by sirtuins, and metabolic and disease implications. *Cell Metab.* **2018**, *27*, 497-512.

12. Christensen, D. G.; Baumgartner, J. T.; Xie, X.; Jew, K. M.; Basisty, N.; Schilling, B.; Kuhn, M. L.; Wolfe, A. J. Mechanisms, detection, and relevance of protein acetylation in prokaryotes. *MBio* **2019**, *10*, pii: e02708-18.

13. Wagner, G. R.; Bhatt, D. P.; O'Connell, T. M.; Thompson, J. W.; Dubois, L. G.; Backos, D. S.; Yang, H.; Mitchell, G. A.; Ilkayeva, O. R.; Stevens, R. D.; Grimsrud, P. A.; Hirschey, M. D. A class of reactive acyl-CoA species reveals the non-enzymatic origins of protein acylation. *Cell Metab.* **2017**, *25*, 823-837.

14. James, A. M.; Hoogewijs, K.; Logan, A.; Hall, A. R.; Ding, S.; Fearnley, I. M.; Murphy, M. P. Non-enzymatic N-acetylation of lysine residues by acetyl-CoA often occurs via a proximal S-acetylated thiol intermediate sensitive to glyoxalase II. *Cell Rep.* **2017**, *18*, 2105-2112.

15. Simic, Z.; Weiwad, M.; Schierhorn, A.; Steegborn, C.; Schutkowski, M. The  $\epsilon$ -amino

- group of protein lysine residues is highly susceptible to nonenzymatic acylation by several physiological acyl-CoA thioesters. *Chembiochem* **2015**, *16*, 2337-2347.
16. Wagner, G. R.; Payne, R. M. Widespread and enzyme-independent N $\epsilon$ -acetylation and N $\epsilon$ -succinylation of proteins in the chemical conditions of the mitochondrial matrix. *J. Biol. Chem.* **2013**, *288*, 29036-29045.
17. Greiss, S.; Gartner, A. Sirtuin/Sir2 phylogeny, evolutionary considerations and structural conservation. *Mol. Cells* **2009**, *28*, 407-415.
18. Wang, Y.; Yang, J.; Hong, T.; Chen, X.; Cui, L. SIRT2: Controversy and multiple roles in disease and physiology. *Ageing Res. Rev.* **2019**, *55*, 100961.
19. Chang, A. R.; Ferrer, C. M.; Mostoslavsky, R. SIRT6, a mammalian deacylase with multitasking abilities. *Physiol. Rev.* **2020**, *100*, 145-169.
20. Lagunas-Rangel, F. A. Current role of mammalian sirtuins in DNA repair. *DNA Repair (Amst)* **2019**, *80*, 85-92.
21. Kosciuk, T.; Wang, M.; Hong, J. Y.; Lin, H. Updates on the epigenetic roles of sirtuins. *Curr. Opin. Chem. Biol.* **2019**, *51*, 18-29.
22. Min, Z.; Gao, J.; Yu, Y. The roles of mitochondrial SIRT4 in cellular metabolism. *Front. Endocrinol. (Lausanne)* **2019**, *9*, 783.
23. Wu, D.; Li, Y.; Zhu, K. S.; Wang, H.; Zhu, W. G. Advances in cellular characterization of the sirtuin isoform, SIRT7. *Front. Endocrinol. (Lausanne)* **2018**, *9*, 652.
24. Kumar, S.; Lombard, D. B. Functions of the sirtuin deacylase SIRT5 in normal physiology and pathobiology. *Crit. Rev. Biochem. Mol. Biol.* **2018**, *53*, 311-334.
25. Elkhwanky, M. S.; Hakkola, J. Extranuclear sirtuins and metabolic stress. *Antioxid. Redox.*

*Signal*. **2018**, *28*, 662-676.

26. Bringman-Rodenbarger, L. R.; Guo, A. H.; Lyssiotis, C. A.; Lombard, D. B. Emerging roles for SIRT5 in metabolism and cancer. *Antioxid. Redox. Signal*. **2018**, *28*, 677-690.

27. Sebastián, C.; Mostoslavsky, R. The role of mammalian sirtuins in cancer metabolism. *Semin. Cell Dev. Biol.* **2015**, *43*, 33-42.

28. Choi, J. E.; Mostoslavsky, R. Sirtuins, metabolism, and DNA repair. *Curr. Opin. Genet. Dev.* **2014**, *26*, 24-32.

29. Wang, Y.; He, J.; Liao, M.; Hu, M.; Li, W.; Ouyang, H.; Wang, X.; Ye, T.; Zhang, Y.; Ouyang, L. An overview of sirtuins as potential therapeutic target: structure, function and modulators. *Eur. J. Med. Chem.* **2019**, *161*, 48-77.

30. Neo, S. H.; Tang, B. L. Sirtuins as modifiers of huntington's disease (HD) pathology. In *Progress in Molecular Biology and Translational Science. Sirtuins in Health and Disease*; 1st ed.; Zheng, W., Ed.; Academic Press: Cambridge, MA, USA, 2018; Volume 154, pp. 105-145.

31. Schiedel, M.; Robaa, D.; Rumpf, T.; Sippl, W.; Jung, M. The current state of NAD<sup>+</sup>-dependent histone deacetylases (sirtuins) as novel therapeutic targets. *Med. Res. Rev.* **2018**, *38*, 147-200.

32. Jiang, Y.; Liu, J.; Chen, D.; Yan, L.; Zheng, W. Sirtuin inhibition: strategies, inhibitors, and therapeutic potential. *Trends Pharmacol. Sci.* **2017**, *38*, 459-472.

33. Wang, T.; Xu, Z.; Lu, Y.; Shi, J.; Liu, W.; Zhang, C.; Jiang, Z.; Qi, B.; Bai, L. Recent progress on the discovery of sirt2 inhibitors for the treatment of various cancers. *Curr. Top. Med. Chem.* **2019**, *19*, 1051-1058.

34. Dai, H.; Sinclair, D. A.; Ellis, J. L.; Steegborn, C. Sirtuin activators and inhibitors: promises, achievements, and challenges. *Pharmacol. Ther.* **2018**, *188*, 140-154.
35. Chen, D.; Zheng, W. Cyclic peptide-based potent and selective SIRT1/2 dual inhibitors harboring N<sup>ε</sup>-thioacetyl-lysine. *Bioorg. Med. Chem. Lett.* **2016**, *26*, 5234-5239.
36. Fatkins, D. G.; Monnot, A. D.; Zheng, W. Nepsilon-thioacetyl-lysine: a multi-facet functional probe for enzymatic protein lysine Nepsilon-deacetylation. *Bioorg. Med. Chem. Lett.* **2006**, *16*, 3651-3656.
37. Tickler, A. K.; Barrow, C. J.; Wade, J. D. Improved preparation of amyloid-beta peptides using DBU as Nalpha-Fmoc deprotection reagent. *J. Pept. Sci.* **2001**, *7*, 488-494.
38. Hong, J. Y.; Zhang, X.; Lin, H. HPLC-based enzyme assays for sirtuins. *Methods Mol. Biol.* **2018**, *1813*, 225-234.
39. Hirsch, B. M.; Gallo, C. A.; Du, Z.; Wang, Z.; Zheng, W. Discovery of potent, proteolytically stable, and cell permeable human sirtuin peptidomimetic inhibitors containing N<sup>ε</sup>-thioacetyl-lysine. *Med. Chem. Comm.* **2010**, *1*, 233-238.
40. Li, S.; Wu, B.; Zheng, W. Cyclic tripeptide-based potent human SIRT7 inhibitors. *Bioorg. Med. Chem. Lett.* **2019**, *29*, 461-465.
41. Dixon, M. The determination of enzyme inhibitor constants. *Biochem. J.* **1953**, *55*, 170-171.
42. George, J.; Nihal, M.; Singh, C. K.; Ahmad, N. 4'-Bromo-resveratrol, a dual sirtuin-1 and sirtuin-3 inhibitor, inhibits melanoma cell growth through mitochondrial metabolic reprogramming. *Mol. Carcinog.* **2019**, *58*, 1876-1885.
43. Nguyen, G. T.; Gertz, M.; Steegborn, C. Crystal structures of sirt3 complexes with

- 4'-bromo-resveratrol reveal binding sites and inhibition mechanism. *Chem. Biol.* **2013**, *20*, 1375-1385.
44. Huang, Y.; Liu, J.; Yan, L.; Zheng, W. Simple N<sup>ε</sup>-thioacetyl-lysine-containing cyclic peptides exhibiting highly potent sirtuin inhibition. *Bioorg. Med. Chem. Lett.* **2016**, *26*, 1612-1617.
45. Smith, B. C.; Denu, J. M. Mechanism-based inhibition of Sir2 deacetylases by thioacetyl-lysine peptide. *Biochemistry* **2007**, *46*, 14478-14486.
46. Goodman, M.; Ro, S. Peptidomimetics for drug design. In *Burger's Medicinal Chemistry and Drug Discovery. Principles and Practice*, 5th ed.; Wolff, M.E., Ed.; John Wiley & Sons: Hoboken, NJ, USA, 1995; Volume 1, pp. 803-861.
47. Avalos, J. L.; Celic, I.; Muhammad, S.; Cosgrove, M. S.; Boeke, J. D.; Wolberger, C. Structure of a Sir2 enzyme bound to an acetylated p53 peptide. *Mol. Cell* **2002**, *10*, 523-535.
48. Zheng, W. Mechanism-based modulator discovery for sirtuin-catalyzed deacetylation reaction. *Mini Rev. Med. Chem.* **2013**, *13*, 132-154.
49. Tyndall, J. D.; Reid, R. C.; Tyssen, D. P.; Jardine, D. K.; Todd, B.; Passmore, M.; March, D. R.; Pattenden, L. K.; Bergman, D. A.; Alewood, D.; Hu, S. H.; Alewood, P. F.; Birch, C. J.; Martin, J. L.; Fairlie, D. P. Synthesis, stability, antiviral activity, and protease-bound structures of substrate-mimicking constrained macrocyclic inhibitors of HIV-1 protease. *J. Med. Chem.* **2000**, *43*, 3495-3504.
50. Reid, R. C.; March, D. R.; Dooley, M. J.; Bergman, D. A.; Abbenante, G.; Fairlie, D. P. A novel bicyclic enzyme inhibitor as a consensus peptidomimetic for the receptor-bound conformations of 12 peptidic inhibitors of HIV-1 protease. *J. Am. Chem. Soc.* **1996**, *118*,

8511-8517.

51. Tong, Z.; Wang, M.; Wang, Y.; Kim, D. D.; Grenier, J. K.; Cao, J.; Sadhukhan, S.; Hao, Q.; Lin, H. SIRT7 is an RNA-activated protein lysine deacylase. *ACS Chem. Biol.* **2017**, *12*, 300-310.

52. Roche Applied Science. Pronase: Product Description. **2006**, and references cited therein.

53. Vaziri, H.; Dessain, S. K.; Ng Eaton, E.; Imai, S. I.; Frye, R. A.; Pandita, T. K.; Guarente, L.; Weinberg, R. A. hSIR2(SIRT1) functions as an NAD-dependent p53 deacetylase. *Cell* **2001**, *107*, 149-159.

54. Peck, B.; Chen, C. Y.; Ho, K. K.; Di Fruscia, P.; Myatt, S. S.; Coombes, R. C.; Fuchter, M. J.; Hsiao, C. D.; Lam, E. W. SIRT inhibitors induce cell death and p53 acetylation through targeting both SIRT1 and SIRT2. *Mol. Cancer Ther.* **2010**, *9*, 844-855.

55. Disch, J. S.; Evindar, G.; Chiu, C. H.; Blum, C. A.; Dai, H.; Jin, L.; Schuman, E.; Lind, K. E.; Belyanskaya, S. L.; Deng, J.; Coppo, F.; Aquilani, L.; Graybill, T. L.; Cuzzo, J. W.; Lavu, S.; Mao, C.; Vlasuk, G. P.; Perni, R. B. Discovery of thieno[3,2-d]pyrimidine-6-carboxamides as potent inhibitors of SIRT1, SIRT2, and SIRT3. *J. Med. Chem.* **2013**, *56*, 3666-3679.

## Graphical Abstract

**A bicyclic pentapeptide-based highly potent and selective pan-SIRT1/2/3 inhibitor harboring N<sup>ε</sup>-thioacetyl-lysine**

Renwu Li, Lingling Yan, Xun Sun\*, and Weiping Zheng\*

Bicyclic pentapeptide **10** harboring the catalytic mechanism-based SIRT1/2/3 inhibitory warhead N<sup>ε</sup>-thioacetyl-lysine at its central position was found to be a highly potent/selective (*versus* SIRT5/6/7), proteolytically stable, and cell permeable pan-SIRT1/2/3 inhibitor which also exhibited an anti-proliferative effect on the human SK-MEL-2 melanoma cells.

